Nuclear Materials and Energy 9 (2016) 233–236

Contents lists available at ScienceDirect

Nuclear Materials and Energy

journal homepage: www.elsevier.com/locate/nme

Hydrogen retention behavior of beryllides as advanced neutron multipliers

Y. Fujii[a], M. Miyamoto[a,*], Jae-Hwan Kim[b], M. Nakamichi[b], N. Murayoshi[c], H. Iwakiri[d]

[a] Department of Material Science, Shimane University, 1060, Nishikawatu, Matsue 690-8504, Japan
[b] Sector of Fusion Research and Development, Japan Atomic Energy Agency, 2-166 Obuchi, Omotedate, Rokkasho, Aomori 039-3212, Japan
[c] Graduate school of energy science, Kyoto University, Gokasho, Uji, Kyoto 611-0011, Japan
[d] Faculty and Graduate School of Education, University of the Ryukyus, Nishihara, Okinawa 903-0213, Japan

ARTICLE INFO

Article history:
Received 16 November 2015
Revised 28 December 2015
Accepted 3 March 2016
Available online 7 April 2016

Keywords:
Thermal desorption spectroscopy
Transmission electron microscopy
Hydrogen
Be12Ti
Microstructure

ABSTRACT

Beryllium intermetallic compounds (beryllides) are the most promising candidate materials for use as advanced neutron multipliers in future fusion reactors because of their low swelling and high stability at high temperatures. Recently, beryllium–titanium beryllide pebbles such as $Be_{12}Ti$ have been successfully fabricated using a novel granulation process. In this study, the fundamental aspects of the behavior of hydrogen isotopes in $Be_{12}Ti$ pebbles were investigated via thermal desorption spectroscopy and transmission electron microscopy. In addition, atomistic calculations using first principles electronic-structure methods were applied to determine the solution energy of hydrogen in $Be_{12}Ti$. The results showed simpler and weaker hydrogen-trapping efficiency for $Be_{12}Ti$ than for pure Be.

© 2016 The Authors. Published by Elsevier Ltd.
This is an open access article under the CC BY-NC-ND license (http://creativecommons.org/licenses/by-nc-nd/4.0/).

1. Introduction

Advanced neutron multipliers with lower swelling and higher stability at high temperatures are desired for solid breeder blankets of future fusion reactors. Beryllium intermetallic compounds (beryllides) have been considered as advanced neutron multiplication materials because of their advantages, such as higher melting point, lower chemical reactivity, and lower swelling, over beryllium. Therefore, the development of fabrication techniques for beryllides has been pursued [1–4]. Recently beryllium–titanium beryllide pebbles such as $Be_{12}Ti$ have been successfully fabricated using a novel granulation process [5,6].

For the practical use of beryllide pebbles in a future fusion reactor such as the DEMOnstration Power Plant (DEMO), an understanding of the behavior of hydrogen isotopes in the neutron multiplier is critical because it influences the functional maintenance of the materials and the safety of the reactor. In this study, the behavior of hydrogen isotopes in $Be_{12}Ti$ pebbles fabricated using the novel granulation method was investigated and compared with metallic Be pebbles via thermal desorption spectroscopy (TDS). The associated microstructure evolution during annealing was observed using a transmission electron microscope (TEM). In addition, the hydrogen positions and solution energies in $Be_{12}Ti$ were investigated using atomistic calculations based on first principles.

2. Experimental procedure

Samples used in this study were pebble-type pure Be and $Be_{12}Ti$ with a diameter of less than 1 mm. These samples were fabricated using newly developed methods combining plasma sintering and rotating electrode methods.

To investigate the characteristics of the hydrogen retention behavior in these samples, TDS was applied after low-energy deuterium ion irradiation without having to change the spherical shapes of the pebble samples. The irradiation was carried out with 3 keV D_2^+ ions (corresponding to 1.5 keV D^+) using fluences in the range of 1×10^{21} to 1×10^{23} D/m^2 at room temperature. The depth distributions of damage and ion range were calculated for this irradiation condition by TRIM-code, and the peak depths of them were estimated to be about 25 and 40 nm, respectively, for both pure Be and $Be_{12}Ti$. While it does not necessarily simulate a particle load under a fusion plasma condition, an ion energy of 3 keV was applied due to the ion source stability of our irradiation device. It should be noted that a surface effect cannot be totally ignored. After irradiation, the samples were annealed from 300 to 1200 K at a constant heating rate of 1 K/s in a high vacuum and the released D_2 was monitored using a quadruple mass spectrometer (QMS). The QMS signals were calibrated using a standard leak

* Corresponding author.
E-mail address: miyamoto@riko.shimane-u.ac.jp (M. Miyamoto).

http://dx.doi.org/10.1016/j.nme.2016.03.001
2352-1791/© 2016 The Authors. Published by Elsevier Ltd. This is an open access article under the CC BY-NC-ND license (http://creativecommons.org/licenses/by-nc-nd/4.0/).

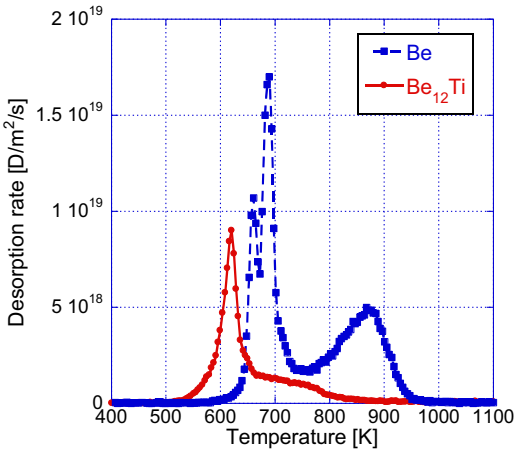

Fig. 1. Thermal desorption spectra of deuterium from $Be_{12}Ti$ and pure Be irradiated with 3 keV D_2^+ at a fluence of 1×10^{22} D^+/m^2 at room temperature.

bottle to quantitatively estimate the deuterium-retention behavior. In addition to the constant heating rate for TDS, the dependence of the heating rates in the range of 0.1–10 K/s was also evaluated to estimate the apparent activation energies of deuterium desorption.

The corresponding microstructure evolution induced by irradiation with 3 keV D_2^+ and the subsequent annealing was examined using an in situ TEM (JEOL-JEM2010) equipped with an ion gun. The focused ion beam technique was applied to prepare the samples from the beryllide pebbles for in situ TEM observation.

3. Calculation details

The solution energy of hydrogen in $Be_{12}Ti$ was investigated with atomistic calculations using first principles electronic-structure methods. The calculation was performed using the density functional theory method as implemented in SIESTA [7]. The electron exchange and correlation were treated with a generalized gradient approximation of the Wu–Cohen modification of the Perdew–Burke–Ernzerh function [8]. The electron–ion interactions were described by norm-conserving Troullier–Martins pseudopotentials. The valence wave functions were expanded in a basis set of localized atomic orbitals. We used double-ζ bases with polarization orbitals in the Be2s, 2p, 3d, 4f, and Ti4s, 4p, 3d, 4f channels. The calculations were carried out in a super-cell containing 52 atoms (48Be+4Ti). The convergence of the calculations was tested, and we determined that a $4 \times 4 \times 4$ k-point grid and a 200 Ry cutoff for the real space mesh produced well-converged results. Relaxation was performed until all Hellmann–Feynman forces converged to 0.01 eV/Å.

The solution energy ΔE_s of a hydrogen atom was defined using the following equation:

$$\Delta E_s = E(Be_{12}Ti - H) - E(Be_{12}Ti) - 1/2E(H_2), \quad (1)$$

where $E(Be_{12}Ti\text{-}H)$, $E(Be_{12}Ti)$, and $E(H_2)$ are the total energies of the system for hydrogen in $Be_{12}Ti$, the perfect $Be_{12}Ti$ crystal, and the hydrogen molecule, respectively.

4. Results and discussions

The thermal desorption experiments exhibited key differences between Be and $Be_{12}Ti$ pebbles. Fig. 1 shows the deuterium desorption spectra from Be and $Be_{12}Ti$ irradiated with 3 keV D_2^+ at a fluence of 1×10^{22} D^+/m^2 at room temperature. While two clear desorption peaks occurred at a high temperature of 870 K and a low temperature of 680 K for pure Be, it was found that, for $Be_{12}Ti$, only a smaller peak at a low temperature of around 620 K was present, accompanied by a tail extending to higher temperatures. Concerning desorption from pure Be, several authors have reported that the lower and higher temperature desorption peaks are related to beryllium hydride [9] and cavities filled with D_2 [10,11], respectively.

The microstructure evolution obtained by in situ TEM observation, which is closely related to the thermal desorption spectra, promoted an understanding of the retention mechanism. This observation also showed the clear difference between the behavior of deuterium bubbles for Be and $Be_{12}Ti$. Fig. 2 shows the microstructure evolution during annealing for pre-thinned Be and $Be_{12}T$ irradiated with 3 keV deuterium ions at a fluence of 1×10^{21} D^+/m^2 at room temperature. For both samples, fine and highly dense deuterium bubbles began to be observed at a fluence of $\sim 10^{21}$ D^+/m^2. The bubbles in Be exhibited significant growth with an increasing temperature of up to 773 K before finally disappearing at ~873 K. As reported elsewhere [10], the desorption peak observed in Be at higher temperatures seems to be attributed to the release from the large deuterium bubbles. On the other hand, the bubbles in $Be_{12}Ti$ gradually shrunk at above 673 K without obvious growth and completely disappeared at above 773 K. This result indicates that the main peak observed in the TDS measurement for $Be_{12}Ti$ at a relatively lower temperature is associated with desorption from the fine bubbles.

To estimate the apparent activation energies of deuterium desorption, the dependence of the heating rates in the range of 0.1–10 K/s was evaluated. For a simple desorption model, the desorption rate of deuterium $N(t)$ can be expressed as

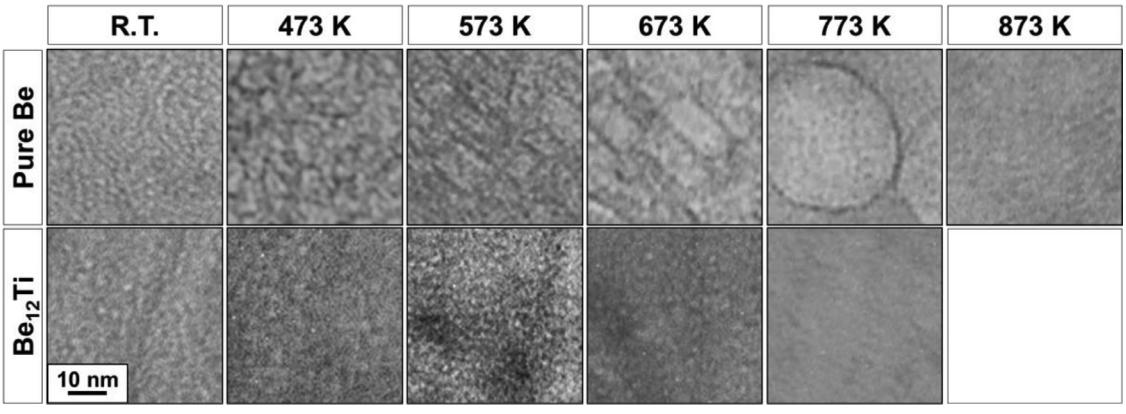

Fig. 2. Microstructure evolution during annealing for pure Be and $Be_{12}Ti$ pre-irradiated with 3 keV D_2^+ at a fluence of 1×10^{21} D^+/m^2 at room temperature.

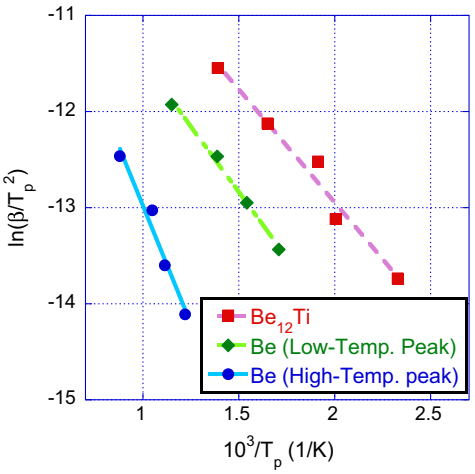

Fig. 3. Arrhenius plot for pure Be and $Be_{12}Ti$.

$$N(t) = d\sigma/dt = -\nu_n \sigma^n \exp(-E/kT), \quad (2)$$

where σ is the surface coverage, n is the order of the desorption reaction, ν_n is the rate constant, k is the Boltzmann constant, and E is the apparent activation energy of desorption [12]. The relationships among the desorption peak temperature T_p, heating rate β, and apparent activation energy E can be expressed without depending on n as

$$\ln(\beta/T_p^2) = -E/kT_p - \ln(E/k\nu). \quad (3)$$

Fig. 3 shows the Arrhenius plot for pure Be and $Be_{12}Ti$. In this plot, the accidental errors were not taken into consideration, since each data was obtained by one measurement. Using Eq. (3), the activation energies were estimated to be 0.23 ± 0.01 and 0.42 ± 0.05 eV for the low and high temperature peaks in Be, respectively, and 0.20 ± 0.02 eV for the peak in $Be_{12}Ti$. This result quantitatively indicates a weaker trapping efficiency of deuterium in $Be_{12}Ti$ compared with Be.

In addition to the experimental measurements, we studied the energetics of interstitial hydrogen in $Be_{12}Ti$ with atomistic calculations using first principles electronic-structure methods.

Parameters designed to optimize the lattice constants by varying the lattice constants and axial ratio (ratio between a-axis and c-axis) based on first principles were deduced to be $a = b = 7.625$ Å and $c = 4.319$ Å. These values were similar to the experimental values of $a = b = 7.360$ Å and $c = 4.195$ Å [13], thus demonstrating the validity of the calculations.

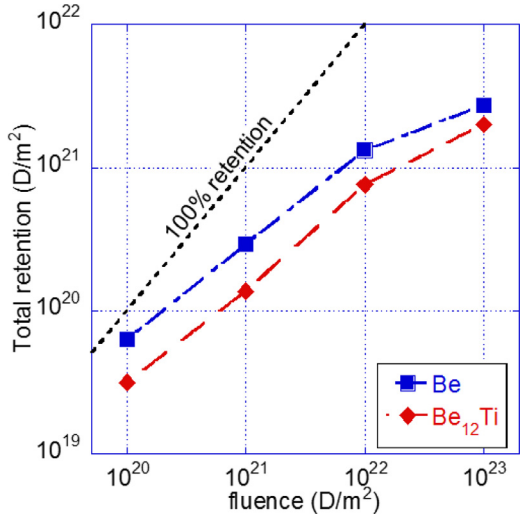

Fig. 5. Total retention of deuterium in pure Be and $Be_{12}Ti$ as a function of the fluence of 3 keV D_2^+.

To investigate the hydrogen solution state in the $Be_{12}Ti$ supercell, 20 sets of lattice sites were chosen for the initial location of a hydrogen atom.

After relaxation, we found six interstitial sites of H in $Be_{12}Ti$ as follows: the interstice of the formal Be_4Ti_2 octahedron (O-site), Be_3Ti tetrahedron (T1-site), Be_4Ti trigonal-dipyramid (TD1-site), Be_8 dodecahedron (D-site), Be_5trigonal-dipyramid (TD2 site), and Be_4 tetrahedron (T2-site). The atomic configurations of these six interstitial sites are shown in Fig. 4 and the solution energies are listed in Table 1.

Since the solution energies show positive values for each configuration, it can be said that $Be_{12}Ti$ is an endothermic hydrogen-occluding metal, i.e., hydrogen does not effectively form a solid solution in $Be_{12}Ti$ unless there are pre-existing defects.

The results thus far indicate a weaker trapping efficiency of hydrogen in $Be_{12}Ti$ than in pure Be. Due to this weak trapping efficiency, the total deuterium retention in $Be_{12}Ti$ is smaller than that in pure Be. Fig. 5 shows the total retention of deuterium in pure Be and $Be_{12}Ti$ as a function of the fluence of 3 keV D_2^+. The retention of $Be_{12}Ti$ was evaluated to be less than half of that in pure Be over a fluence range of 10^{20} to 10^{23} D^+/m^2. In this respect, as

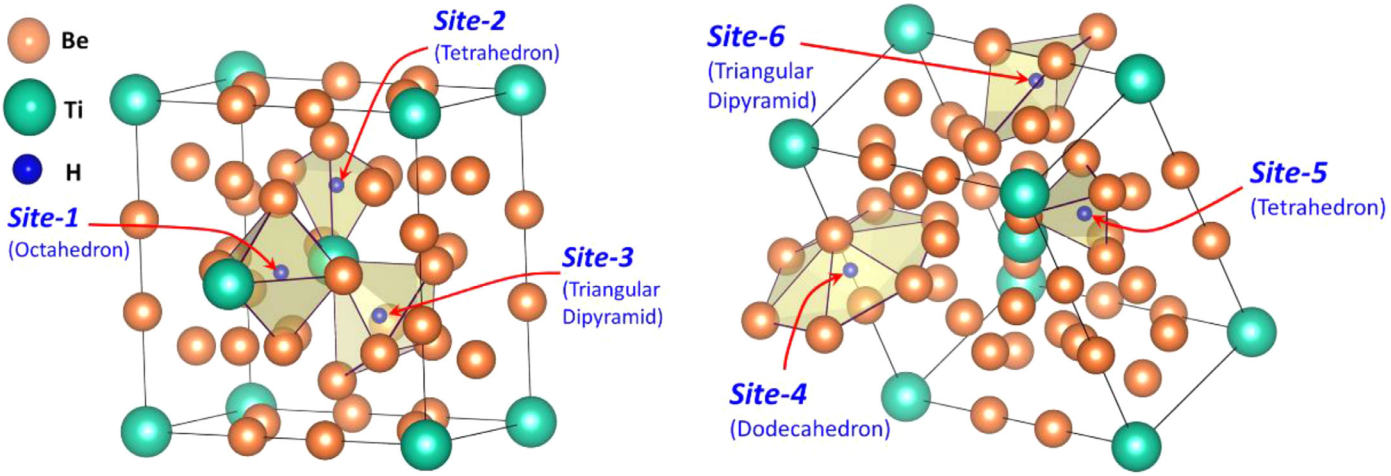

Fig. 4. Six energetically favorable configurations of a hydrogen atom in $Be_{12}Ti$.

Table 1
Solution energies of hydrogen for available sites in the $Be_{12}Ti$ structure.

Site- 1 O (Be_4Ti_2)	Site-2 T1 (Be_3Ti)	Site- 3 TD1 (Be_4Ti)	Site- 4 DOD (Be_8)	Site- 5 TD2 (Be_6)	Site- 6 T2 (Be_4)
+0.11 eV	+0.27 eV	+0.33 eV	+0.52 eV	+0.85 eV	+1.06 eV

a neutron multiplier, the newly developed $Be_{12}Ti$ pebbles exhibit better performance than pure Be pebbles. To understand the usage condition of $Be_{12}Ti$ pebbles, the effects of irradiation temperature and the additional influence of transmuted helium on the hydrogen retention property will be studied in future work.

5. Summary

The hydrogen retention behavior in $Be_{12}Ti$ pebbles for use as advanced neutron multipliers was investigated by TDS and TEM observation for comparison with pure Be pebbles. In addition, atomistic calculations using first principles electronic-structure methods were applied. The following results were obtained.

1. The TDS results imply a simpler and weaker retention mechanism for $Be_{12}Ti$ than for metallic Be.
2. The apparent activation energies of hydrogen desorption in $Be_{12}Ti$ were estimated to be 0.20 eV, which is much lower than that for metallic Be.
3. Results from the first principles electronic-structure method indicate that $Be_{12}Ti$ is an endothermic hydrogen-occluding metal, i.e., hydrogen does not effectively form a solid solution in $Be_{12}Ti$ unless there are pre-existing defects.

As a result, $Be_{12}Ti$ pebbles are superior to Be pebbles from the viewpoint of hydrogen retention behavior.

Acknowledgment

The authors wish to thank JAEA technical staffs for their professional skill and dedicated support. This work was partly supported by JAEA under the Joint Work contract 27K414, as a part of Broader Approach activities and a Grant-in-Aid for Young Scientists (A) 25709086 from the Japan Society for the Promotion of Science (JSPS).

References

[1] E. Ishitsuka, et al., Fusion Eng. Des. 27 (1995) 263–268.
[2] Y. Mishima, et al., Fusion Eng. Des. 82 (2007) 91–97.
[3] M. Nakamichi, et al., J. Nucl. Mater. 417 (2011) 765–768.
[4] M. Nakamichi, et al., J. Nucl. Mater. 442 (2013) S465–S471.
[5] M. Nakamichi, et al., J. Nucl. Mater. 440 (2011) 530–533.
[6] J.-H. Kim, et al., J. Alloys Compd. 585 (2014) 63–68.
[7] E. Artacho, et al., Phys. Status Solidi B 215 (1999) 809.
[8] Z. Wu, R.E. Cohen, Phys. Rev. B 73 (2006) 235116.
[9] K.L. Wilson, et al., J. Vac. Sci. Technol. A 8 (1990) 1750–1759.
[10] W.R. Wampler, J. Nucl. Mater. 196-198 (1992) 981–985.
[11] V. Kh. Alimov, J. Nucl. Mater. 241-243 (1997) 1047–1051.
[12] P.A. Redhead, Vacuum 12 (1962) 203–211.
[13] E. Gillam, H.P. Rooksby, L.D. Brownlee, ActaCryst 17 (1964) 762–763.